

Tight Junction Modulatory Fusion Peptide (ADT-6) Enhances GFP Protein Permeability through the Paracellular Pathway in Caco-2 Cell Lines: An *In-Vitro* Study

Salimeh Hassani¹, Keyvan Nedaei¹, Rahim Jafari², Ghasem Bagherpour*³

Abstract

Background: The oral delivery of therapeutic peptides and proteins presents a significant challenge in pharmaceutical development due to barriers such as the intestinal epithelium and the blood-brain barrier (BBB). These barriers limit the passage of large, hydrophilic molecules through transcellular pathways and restrict paracellular transport due to intercellular tight junctions. This study investigates the potential of E-cadherin-modulating peptide, ADT-6, to improve the penetration of these therapeutic agents.

Methods: We constructed a fusion protein of ADT-6 and green fluorescent protein (GFP) to evaluate its activity and transport through the epithelial cells' paracellular pathway. Using Escherichia coli strains for expression, we cloned the GFP-ADT-6 construct, which provides a solid foundation for our study's methodology.

Results: Our molecular simulations showed that the linker between GFP and ADT-6 maintains the fusion protein's integrity and provides flexibility in receptor interaction. Permeability experiments revealed that ADT-6 markedly reduced transepithelial electrical resistance (TEER) and significantly increased GFP transfection in Caco-2 cell monolayers dose-dependently. Results of ELISA confirmed these findings, showing high GFP levels in the lower compartment of Transwell systems treated with GFP-ADT-6.

Conclusions: This study demonstrates the potential of ADT-6 to deliver proteins from the paracellular route, enhance the bioavailability of pharmaceutical drugs by altering cell-cell interactions, and provide new opportunities for oral drug delivery strategies.

Keywords: Caco-2 cells, Tight Junctions, Permeability, Recombinant fusion protein.

Introduction

Delivering peptides and therapeutic proteins orally has always been a goal in pharmaceutical development because it is both convenient for patients and increases compliance. Nevertheless, achieving efficient oral bioavailability is difficult because of the biological obstacles posed by the intestinal and nasal epithelium as well as the blood-brain barrier (BBB). These barriers typically comprise cell membranes formed by cells with

intercellular junctions (1, 2). Due to their size and hydrophilic nature, peptides and proteins cannot cross these barriers through transcellular pathways. Alternatively, these molecules can be transported via paracellular pathways; however, the paracellular transport of peptides and proteins is restricted by tight intercellular junctions. These tight junctions have minimal porosity (<10 Å), permitting only small molecules and ions to pass through

1: Department of Medical Biotechnology, Faculty of Medicine, Zanjan University of Medical Sciences, Zanjan, Iran.

2: Nanotechnology Research Center, Zanjan University of Medical Sciences, Zanjan, Iran.

3: Zanjan Pharmaceutical Biotechnology Research Center, Zanjan University of Medical Sciences, Zanjan, Iran.

*Corresponding author: Ghasem Bagherpour; Tel: +98 24 33140340; E-mail: g_bagherpour@zums.ac.ir.

Received: 17 Sep, 2024; Accepted: 10 Nov, 2024

(3, 4). Therefore, strategies should be developed to improve the transport of more hydrophilic molecules, such as peptides and proteins. One way to achieve this goal is to increase the permeability of intercellular junctions by modulating protein-protein interactions, especially those involving E-cadherins (5, 6). E-cadherin modulatory peptide modifies the porosity of tight intercellular junctions by inhibiting E-cadherin-E-cadherin interactions. These interactions can be interrupted by using small peptides derived from the sequences of the contact (bulge and groove) regions of E-cadherins (7, 8). E-cadherins are a group of transmembrane glycoproteins located in the zonula adherens (adherens junction), positioned between tight junctions (zonula occludens) and desmosomes (9-11).

Previous studies have demonstrated that several peptides, including C-CPE, AT-1002, HAV-6, ADT-6, and PN159 peptides, can enhance the permeability of therapeutic proteins in both intestinal epithelial cells and the Blood-Brain Barrier (BBB) endothelial cells with different targeting molecules in the tight junction (12). The peptide ADT-6 (Ac-ADTPPV-NH₂) is a hexapeptide that enhances the release of drugs by modulating cell adhesion properties. This peptide targets the extended regions of the first extracellular domain of E-cadherin (EC-1) and disrupts its hemophilic binding (13). In prior research, the ADT-6 peptide was synthesized and utilized independently as a modulator to enhance permeability in Caco-2 cells (14). In the present study, we fused the peptide to GFP as a marker and model protein to investigate its ability to retain functionality while facilitating the passage of the fusion protein through epithelial cells. The potential of ADT-6 in drug delivery is promising and offers innovative ways to increase the bioavailability of therapeutic agents.

Materials and Methods

Strains and Plasmids

Escherichia coli strains Top 10F' and BL21 (DE3) were utilized as hosts for plasmid

preparations and the expression of the GFP-ADT-6 protein, respectively. The pET28-GFP plasmid (Addgene plasmid #60733) was employed to amplify GFP. Luria-Bertani (LB) medium, with or without agar, supplemented with kanamycin (50 mg/ml), served as the selection medium during the cloning and expression processes.

Molecular Dynamics Simulation

The model of ADT-6 attached to GFP via a 7-glycine linker was constructed using MODELLER version 10.4, with PDB structure 3G9A as the template (15). The model-building process was facilitated by EasyModeller (16). Molecular dynamics simulations of the modeled protein were conducted using GROMACS software version 2021, employing the CHARMM36 force field (17). The protein was solvated in a cubic box with dimensions of 9.5 nm × 9.5 nm × 9.5 nm, utilizing the TIP3P water model. To achieve physiological ionic concentration and neutralize the system's charge, a total of 76 sodium ions and 70 chloride ions were added. Periodic boundary conditions (PBC) were applied in all dimensions. A distance cutoff of 1.2 nm was set for electrostatic and van der Waals interactions, with the Particle Mesh Ewald (PME) method employed to handle long-range electrostatic interactions. For distances ranging from 1.0 to 1.2 nm, van der Waals forces were smoothly turned off using a switch function. The LINCS algorithm was utilized to constrain bonds involving hydrogen atoms, enabling an integration time step of 2 fs. Both equilibration and production simulations were conducted in the NPT ensemble, maintaining the system temperature at 310 K and pressure at 1 bar using the Nose-Hoover thermostat and Parrinello-Rahman barostat, respectively. Following a one ns equilibration period, the molecular dynamics simulation was executed for 100 ns, with system coordinates saved every ten ps. The resulting trajectory was visually analyzed using VMD software (18).

Bioinformatics Studies and Primer Design

The primer sequences employed in this study were meticulously designed using Snap Gene version 3.2.1 and CLC Genomics Workbench 10. Following the design process, the primers were synthesized by Metabion International AG, Germany (Table 1). The GFP sequence was sourced from the pET28-GFP plasmid. The reverse primer was designed to include the ADT-6 sequence, the linker sequence (G6) (19, 20), and the *SacI* restriction site, whereas the forward primer contained only the *EcoRI* restriction site (Fig. 1).

Table 1. Primer list used in PCR for amplification of GFP-ADT-6 cassette.

Primer Name	Sequence 5'-3'
F GFP-G6-ADT-6 (<i>EcoRI</i>)	TATGAGCTCTTACACCGGC GGGGTATCCGCGCCGCCG CCGCCGCCGCCATGTG TAATCCCAGCAG
R GFP (<i>SacI</i>)	GAATTCAAAGGAGAAGAA CTTTCACTGG

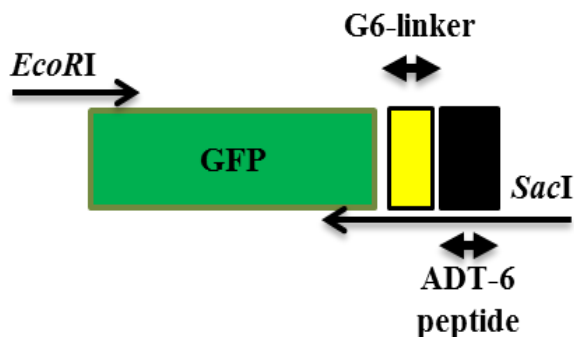


Fig. 1. GFP-ADT-6 construct. G6-Linker and ADT-6 peptide incorporated in the reverse primer

Construction of the pET28-GFP-ADT-6 Cassette

The plasmid pET28-GFP was used as the PCR template to amplify the GFP gene. PCR products and the pET-28 vector were digested with *EcoRI* and *SacI* enzymes. After overnight ligation at 4 °C, the ligation mixture was introduced into competent *E. coli* Top 10F' cells using the CaCl₂. Confirmation of the pET28-GFP-ADT-6 cloning was achieved through colony PCR, restriction digestion, and

sequencing. Subsequently, this plasmid and the control plasmid (pET28-GFP) were expressed in BL21 (DE3) cells.

Protein Expression Analysis and Quantification

For expression analysis of recombinant GFP (with or without ADT-6), BL21 transformants were cultivated in 5 ml of LB broth supplemented with kanamycin (50 mg/ml) and incubated at 37 °C with shaking overnight. Following incubation, the bacterial pellet was collected via centrifugation. The harvested cells were subjected to sodium dodecyl sulfate-polyacrylamide gel electrophoresis (SDS-PAGE) for analysis, and the expression of recombinant GFP was confirmed through Western blotting. A 1:2000 dilution of horseradish peroxidase (HRP)-conjugated His-tag antibody (Sigma-Aldrich) was used to detect immunoreactive bands, with visualization achieved using the colorimetric substrate 3,3'-diaminobenzidine (DAB) (Amersham, USA). Ni-NTA columns were employed for purification and protein quantification, followed by concentration using Amicon columns. The Bradford assay was then performed according to the protocol (21). Finally, the penetration results were assessed using an ELISA test.

Cell Treatment

The Caco-2 cell line was cultured in Dulbecco's Modified Eagle's Medium (DMEM-F12) supplemented with 10% fetal bovine serum (FBS) (Gibco, USA), 50 mg/mL penicillin, and 100 µg/mL streptomycin. The cells were incubated at 37 °C in a humidified atmosphere containing 5% CO₂. Monolayer adherent cells were detached from the flask bottom using an EDTA-trypsin solution. For Transwell experiments, cells were seeded onto 12-well Transwell inserts (SPL #300924, Korea) at a density of 2×10^5 cells per well and allowed to grow until full confluence was reached (approximately 21 days post-plating). The culture medium was refreshed every other day during the first week and daily for the subsequent two weeks.

Paracellular Barrier Integrity Measurement

Transepithelial electrical resistance (TEER) was used to assess the integrity of cell monolayers as described previously (14). A Millicell-ERS volt-ohmmeter (Millipore, Germany) was used to measure the tightness of intercellular junctions. Three concentrations of GFP (with or without ADT-6), specifically 5 and 20 μ g/mL, were freshly prepared, and each well's resistance was measured three times to obtain an average resistance value. Additionally, each experiment included a cell-free blank well for comparison. The electrical resistance of each Transwell was recorded at various time points, ranging from 30 minutes to 48 hours (at 30 minutes, 1 hour, 2 hours, 4 hours, 8 hours, 12 hours, 24 hours, 36 hours, and 48 hours)

The enzyme-linked immunosorbent assay (ELISA)

Caco-2 cells were pretreated with 5 and 20 μ g/mL of GFP (with or without ADT-6) for 48 hours. The concentration of GFP was measured in the lower compartment of the Transwell. Absorbance was recorded at 450 nm using a microplate reader (BioTek Instruments, Inc. USA), with six parallel wells

set up for each ELISA assay.

Statistical Analysis

Statistical analyses were accomplished using Prism version 8 (GraphPad Software, La Jolla, California, USA). The TEER and ELISA data were presented as mean values \pm standard deviation. Intra- and intergroup differences were assessed using one-way analysis of variance (ANOVA), with p-values less than 0.05 considered statistically significant.

Results

Molecular dynamics (MD) Simulation of GFP-ADT-6 Fusion Protein

In a molecular dynamics (MD) simulation lasting 100 nanoseconds, we observed that the amino acids with the highest root mean square fluctuation (RMSF) values were in the linker residues (positions 233-239) and the ADT6 segment (positions 240-245) (Fig. 2). A visual analysis of the trajectory revealed that the structure of the GFP component remained largely stable throughout the simulation period. In contrast, the C-terminal portion of the fusion protein, specifically the ADT6 segment, displayed notable displacements (Fig. 3).

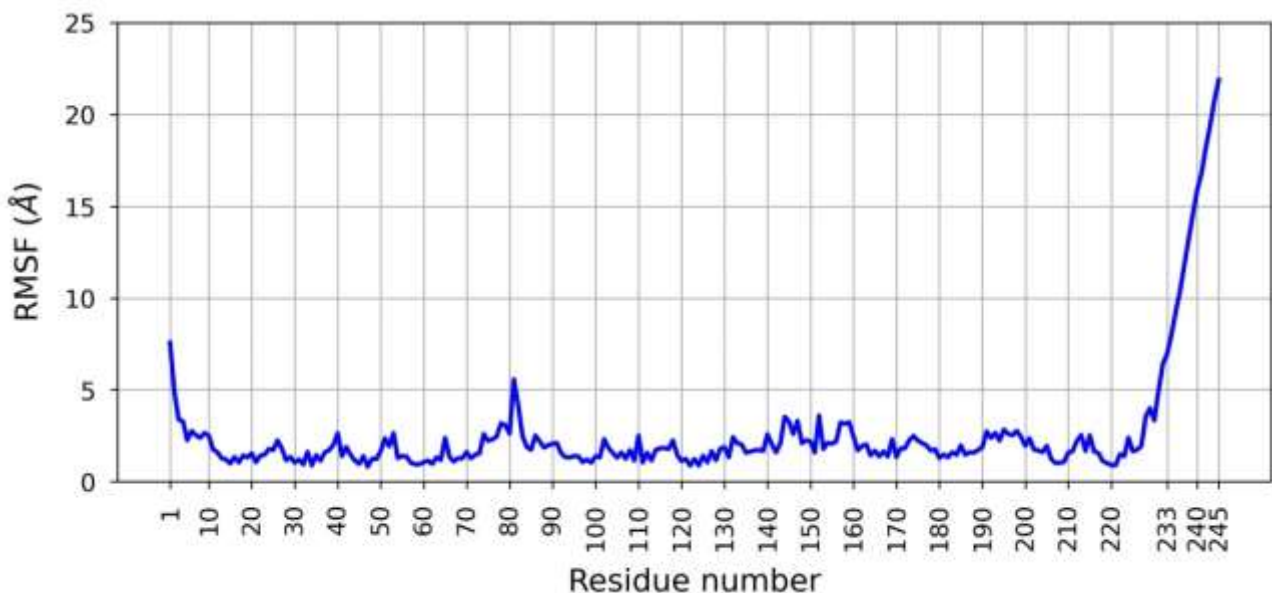


Fig. 2. Root Mean Square Fluctuation (RMSF) of the fusion protein residues for 100 ns MD simulation. Residues 233 to 239 correspond to polyglycine linker and residues 240 to 245 correspond to ADT6 motif.

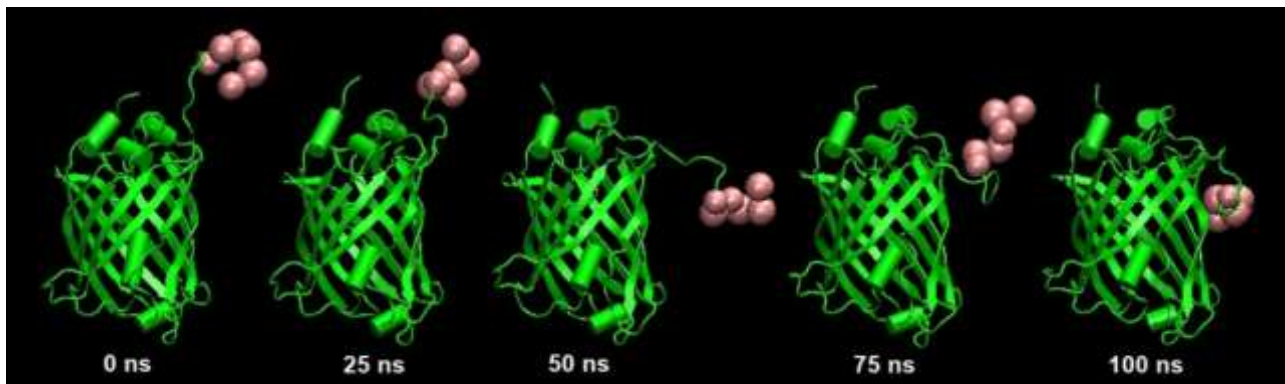


Fig. 3. Snapshots of the fusion protein at different simulation times. The GFP and polyglycine linker are colored in green. The residues of the ADT6 segment are represented as pink beads. During the simulation, the ADT6 moiety underwent numerous big, continuous displacements, but the GFP only had slight structural changes.

Construction of the Cassette and Expression Analysis of GFP-ADT-6 Fusion Protein to confirm the cloning of the GFP gene in the pET-28a (+) plasmid, we performed PCR using specific primers followed by *Eco*RI/*Sac*I digestion. The results confirmed that the gene was inserted correctly. Subsequent sequencing of the pET28-GFP-ADT-6 cassette confirmed its integrity, and no errors were detected.

Fluorescent microscopy at 40X magnification was employed to observe GFP expression in induced *E. coli* BL21 (DE3) cells treated with 1 mM IPTG (Fig. 4A). Additionally, a Western blot analysis of the bacterial lysate and NiNTA-purified GFP-ADT-6 protein (approximately 31 kDa) indicated successful expression and purification of the fusion protein (Fig. 4B).

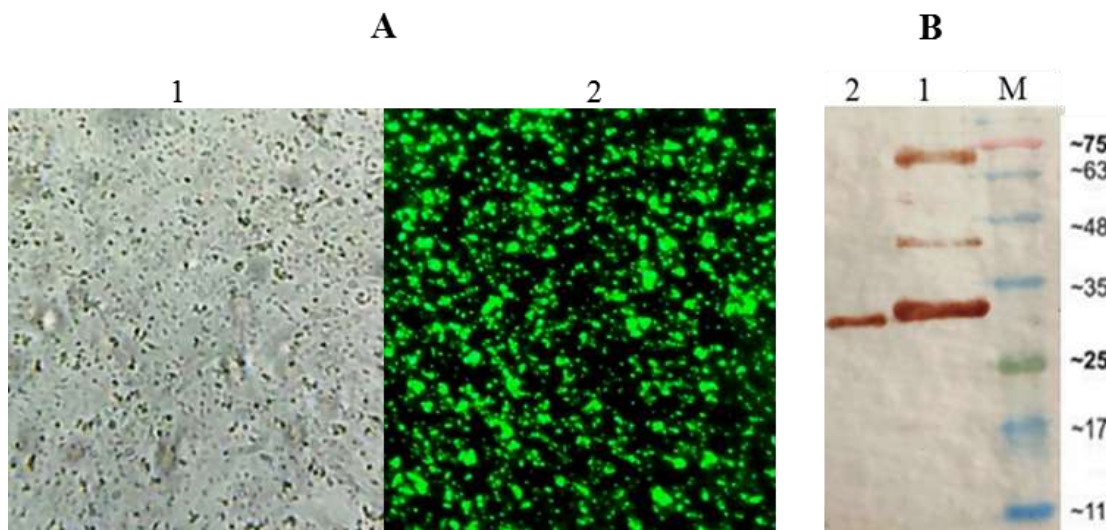


Fig. 4. Fluorescent microscopy (A) and Western blot (B) results. 40X objective lens without UV (A1) and with UV (A2) used for microscopic test. In western blot, lysate (1) and purified (2) GFP-ADT-6 run and detected by his-tag antibody. M, Molecular weight in KD.

Permeability Test

In the Permeability Test, we observed significant differences in the Trans-Epithelial Electrical Resistance (TEER) assay between the test group (GFP-ADT6) and the control (PBS) at a concentration of 5 μ g/ml across various time points. Notably, these differences were evident at 2 hours, between the test and

PBS ($p < 0.05$), and at 4 h differences were between the test and PBS ($P < 0.001$). After 8 h results indicated that the test group had a significant difference with PBS ($p < 0.05$), while in the following hours from 12 h to 48 h, no significant differences were observed between groups (Fig. 5A). At the second

concentration of 20 $\mu\text{g/ml}$, significant differences were also recorded between the test and PBS at 2 hours, as well as between the PBS and both test and GFP at 4 hours, and between

the test and PBS at both 8 and 12 hours ($p < 0.05$) (Fig. 5B). Significantly, we observed the restoration of integrity in all treatment groups after 24 hours.

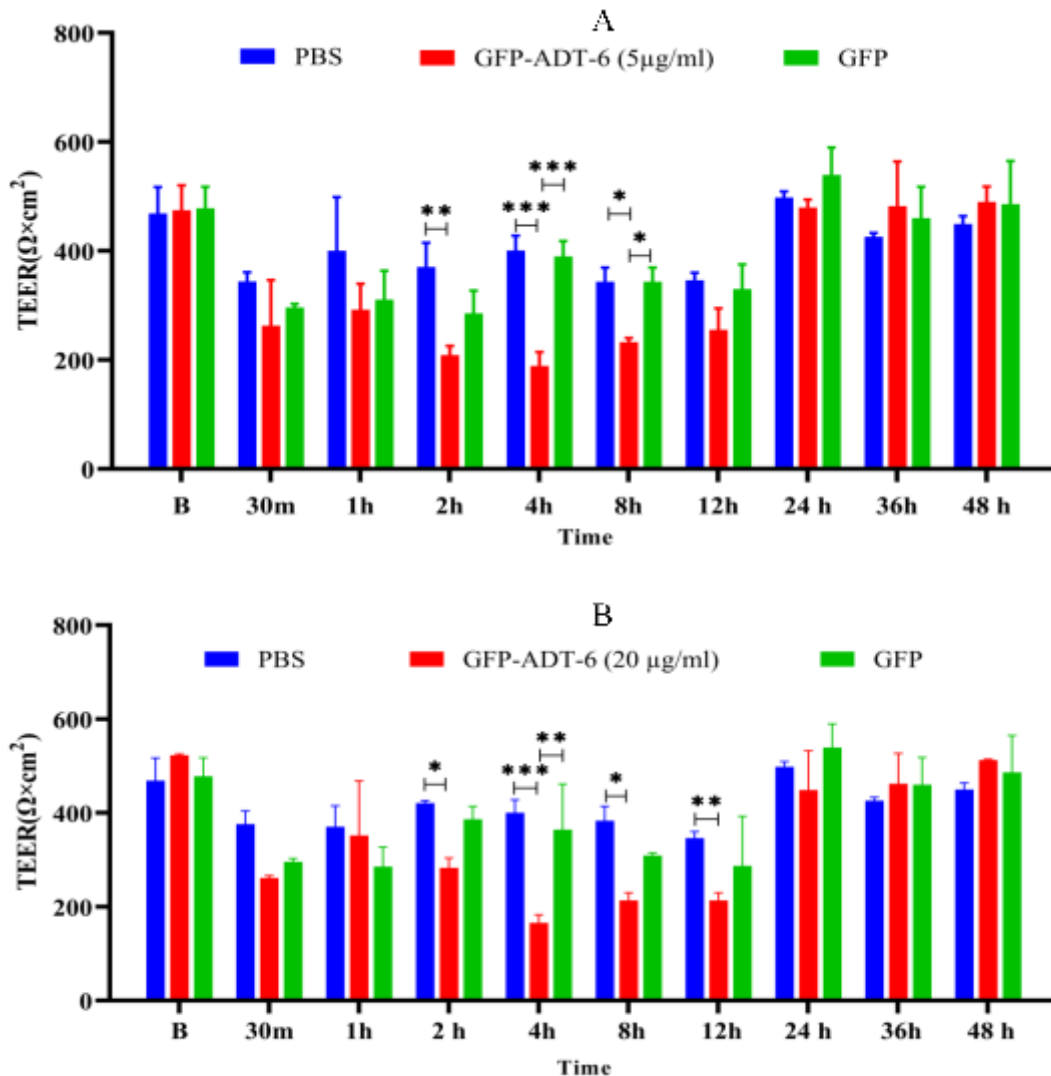


Fig. 5. TEER assay results. CaCo2 cells were treated with GFP-ADT-6 fusion protein in two concentrations. In the first concentration 5 $\mu\text{g/ml}$ (A), differences were at 2 hours, between the test with PBS, at 4 and 8 hours, differences were between the test with PBS and GFP with PBS. In the second concentration 20 $\mu\text{g/ml}$ (B), differences started at 2 hours and terminated at 12 hours. Significant differences were indicated between the test and PBS at 2 hours, as well as between the test with PBS and GFP at 4 hours, and between the test and PBS at both 8 and 12 hours. * $P < 0.05$, ** $P < 0.01$, *** $P < 0.001$.

The enzyme-linked immunosorbent assay (ELISA)

The GFP levels in the lower compartment of the transwell were measured using the ELISA method. Media collected after 4 hours were analyzed at 5 and 20 $\mu\text{g/ml}$ concentrations. The results indicated that GFP-ADT-6 significantly increased permeability at both

concentrations, with p -values of < 0.02 and < 0.002 for 5 and 20 $\mu\text{g/ml}$, respectively, compared to the GFP control. Also, more significant differences were observed between GFP-ADT-6 and PBS, with p -values < 0.003 and < 0.0001 for 5 and 20 $\mu\text{g/ml}$, respectively (Fig. 6).

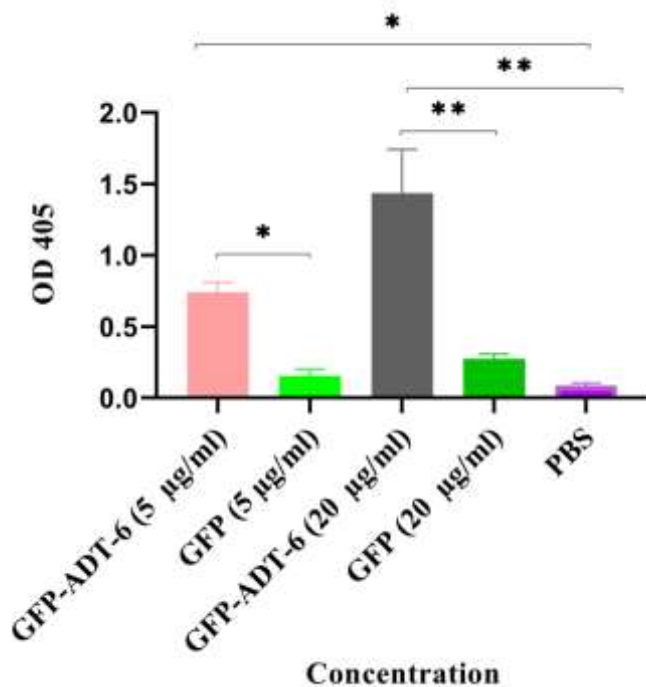


Fig. 6. ELISA results for two concentrations used in the ELISA assay. Significant differences were indicated in both concentrations (5 μ g/ml and 20 μ g/ml) between GFP-ADT-6 and control groups(GFP and PBS). * $P < 0.05$, ** $P < 0.01$, *** $P < 0.001$.

Discussion

In this study, the spatial hindrance of ADT-6 fused to GFP was compared using molecular dynamics to ensure that this peptide is available to its receptor (EC-1) without any problem. The RMSF result, which indicates the fusion protein's flexibility and freedom of movement, showed that regions located in linker residues exhibit the most excellent flexibility and freedom of movement. This result is significant as it suggests that the fusion of ADT6 to GFP through a glycine linker did not significantly impact its biological activity, as ADT6 was free and away from GFP for most of the simulation period, except for some short moments of transient interaction.

Cloning of the GFP-G6-ADT-6 construct into the pET-28 vector was confirmed through molecular methods, followed by expression analysis in BL21 (DE3) cells using Western blotting. The functionality of the GFP-ADT-6 construct was then assessed through a transepithelial electrical resistance (TEER) test. For permeability testing, the resistance of

Caco-2 cell lines was measured using a volt-ohmmeter. Finally, an ELISA was used as a confirmatory test to detect the quantity of GFP-ADT-6 protein in the lower part of the transwells compared to the control group.

The results showed that the fused peptide, like the free synthesized peptide (14), can increase permeability dose-dependently. This result demonstrates the potential of the ADT-6 peptide to enhance the permeability of the fusion protein. Functional tests showed that the ADT-6 peptide increased the permeability of Caco-2 cells for the fusion protein, with a significant increase as the dose increased from 5 μ g/ml to 20 μ g/ml, a significant difference compared to GFP as a control. This result indicates that the ADT-6 peptide, when fused with GFP, can significantly enhance permeability dose-dependently.

In addition to dose effects, paracellular permeability was evaluated over time. Results from the TEER tests on Caco-2 cells revealed that maximum permeability occurred four hours post-treatment for both doses (5 and 20 μ g/ml). Significant differences in permeability

began two hours after treatment with the fusion protein. These differences persisted for eight hours at the 5 μ g/ml concentration, while at 20 μ g/ml, they extended to twelve hours. These findings indicate higher permeability occurs when concentrations increase, with the highest at 20 μ g/ml.

These findings align with previous studies by Sinaga and his colleagues (22), which indicated that the ADT-decapeptide could modulate intercellular junctions from the basolateral side, while the ADT-6 peptide enhanced paracellular permeability. In our study, the fused ADT-6 peptide acted similarly to a free synthetic peptide, enhancing the permeability of the fused GFP. This finding suggests that the ADT-6 peptide, when fused with GFP, can enhance permeability by affecting intercellular junctions. Bocsik's research (23) showed that treatment with a synthetic ADT-6 peptide significantly improved permeability in Caco-2 cells within one hour; however, we observed significant improvements at two hours, with even more pronounced effects at four hours. This

discrepancy may be attributed to the fusion form of ADT-6 utilized in our study.

The reversible interaction of ADT-6 and its ability to enhance intestinal permeability underscore its potential as a safe and promising component for therapeutic applications. The fusion format of ADT-6 can be a game-changer when expressed in some probiotic organisms in oral delivery vehicles and intranasal delivery systems, offering new possibilities for drug delivery.

Acknowledgments

The authors wish to thank the personnel of the Department of Medical Biotechnology, Zanjan University of Medical Sciences for their help and guidance.

Funding

Zanjan University of Medical Sciences, Grant/Award Numbers: A-12-1602-5, Ethical code, IR.ZUMS.AEC.1400.513.

Conflict of interest

No conflict.

References

1. Otani T, Furuse M. Tight Junction Structure and Function Revisited. *Trends Cell Biol.* 2020;30(10):805-817.
2. Zihni C, Mills C, Matter K, Balda MS. Tight junctions: from simple barriers to multifunctional molecular gates. *Nat Rev Mol Cell Biol.* 2016;17(9):564-80.
3. Ma TY, Nighot P, Al-Sadi R. Tight junctions and the intestinal barrier. *Physiology of the Gastrointestinal Tract*: Elsevier; 2018: 587-639.
4. Rosenthal R, Günzel D, Piontek J, Krug SM, Ayala-Torres C, Hempel C, et al. Claudin-15 forms a water channel through the tight junction with distinct function compared to claudin-2. *Acta Physiol (Oxf)*. 2020;228(1):e13334.
5. Brunner J, Ragupathy S, Borchard G. Target specific tight junction modulators. *Adv Drug Deliv Rev.* 2021;171:266-288.
6. Nasir Uddin S, Sultana A, Fatima A, Geethakumari AM, Biswas KH. Regulation of Tight Junction by Cadherin Adhesion and Its Implication in Inflammation and Cancer. *Tight Junctions in Inflammation and Cancer*: Springer; 2023:49-66.
7. Barcelona-Esteve E, Dalby MJ, Cantini M, Salmeron-Sanchez M. You Talking to Me? Cadherin and Integrin Crosstalk in Biomaterial Design. *Adv Healthc Mater.* 2021;10(6):e2002048.
8. Ulapane KR, Kopec BM, Siahaan TJ. Improving In Vivo Brain Delivery of Monoclonal Antibody Using Novel Cyclic Peptides. *Pharmaceutics*. 2019;11(11):568.
9. Horowitz A. Membrane Trafficking of Integral Cell Junction Proteins and its Functional Consequences. 2021; *ArXiv*. <https://arxiv.org/abs/2101.05221>.
10. Ganjare A, Bagul N, Kathariya R, Oberoi J. 'Cell junctions of oral mucosa'-in a nutshell. *QScience Connect*. 2015;2015(1):7.
11. Adil MS, Narayanan SP, Somanath PR. Cell-cell junctions: structure and regulation in physiology and pathology. *Tissue Barriers*. 2021;9(1):1848212.

12. Kiptoo P, Sinaga E, Calcagno AM, Zhao H, Kobayashi N, Tambunan US, Siahaan TJ. Enhancement of drug absorption through the blood-brain barrier and inhibition of intercellular tight junction resealing by E-cadherin peptides. *Mol Pharm.* 2011;8(1):239-49.
13. Kim D, Jin L, Park EJ, Na DH. Peptide permeation enhancers for improving oral bioavailability of macromolecules. *J Pharm Investig.* 2023;53:59-72.
14. Bocsik A, Walter FR, Gyebrovszki A, Fülöp L, Blasig I, Dabrowski S, et al. Reversible Opening of Intercellular Junctions of Intestinal Epithelial and Brain Endothelial Cells with Tight Junction Modulator Peptides. *J Pharm Sci.* 2016;105(2):754-765.
15. Fiser A, Sali A. Modeller: generation and refinement of homology-based protein structure models. *Methods Enzymol.* 2003;374:461-91.
16. Kuntal BK, Aparoy P, Reddanna P. EasyModeller: A graphical interface to MODELLER. *BMC Res Notes.* 2010;3:226.
17. Huang J, MacKerell AD Jr. CHARMM36 all-atom additive protein force field: validation based on comparison to NMR data. *J Comput Chem.* 2013;34(25):2135-45.
18. Humphrey W, Dalke A, Schulten K. VMD: visual molecular dynamics. *J Mol Graph.* 1996;14(1):33-8, 27-8.
19. Soezi M, Memarnejadian A, Aminzadeh S, Zabihollahi R, Sadat SM, Amini S, et al. Toward the development of a single-round infection assay based on EGFP reporting for anti-HIV-1 drug discovery. *Rep Biochem Mol Biol.* 2015;4(1):1-9.
20. Rezaei S, Hadadian S, Khavari-Nejad RA, Norouzian D. Recombinant Tandem Repeated Expression of S3 and S Δ 3 Antimicrobial Peptides. *Rep Biochem Mol Biol.* 2020;9(3):348-356.
21. Kruger NJ. The Bradford method for protein quantitation. *Methods Mol Biol.* 1994;32:9-15.
22. Sinaga E, Jois SD, Avery M, Makagiansar IT, Tambunan US, Audus KL, Siahaan TJ. Increasing paracellular porosity by E-cadherin peptides: discovery of bulge and groove regions in the EC1-domain of E-cadherin. *Pharm Res.* 2002;19(8):1170-9.
23. Bocsik A. Modulation of tight junctions by peptides to increase drug penetration across biological barriers: Szegedi Tudomanyegyetem (University of Szeged, Hungary, Doctoral thesis); 2016.